JTTEE5 19:49–55
DOI: 10.1007/s11666-009-9432-0
1059-9630/$19.00 © ASM International

Alumina Splat Investigation: Visualization of Impact and Splat/Substrate Interface for Millimeter-Sized Drops

S. Goutier, M. Vardelle, J.C. Labbe, and P. Fauchais

(Submitted September 9, 2009; in revised form October 21, 2009)

Coating adhesion-cohesion is strongly linked to the real contact between splats and substrate and between themselves. Unfortunately, the study of a single micrometer-sized splat interface, resulting from flattening and solidification processes and dynamic behaviors, all occurring in a few microseconds, is extremely complex. To overcome problems due to time and dimension scales, many previous works were devoted to the flattening of millimeter-sized drops. However, because of difficulties in producing millimeter-sized ceramic fully melted drops, most works were devoted to metals or alloys. The aim of this work is to present the development of a setup to understand the effect of substrate surface chemistry (oxidation, atom diffusion, etc.) on the flattening of a single millimeter-sized alumina drop. Thus, a new technique to produce such drops with different impact velocities has been developed. It consists in a rotating crucible heated by a transferred arc and a piston controlling substrate velocity and thus drop velocity relative to it. A fast camera (4000 image/s) that combines temperature evolution with a fast pyrometer (4000 Hz), allows following the drop flattening. This system enables the study of interface phenomena (such as desorption of adsorbates and condensates, and liquid drop/substrate wettability) and investigate the effects, at impact, of the kinetic energy or the Weber number of the flattening drop.

Keywords diagnostics and control, preheating of substrates, splats cooling

1. Introduction

The impact of liquid droplets plays an important role in many processes. For example, in plasma spraying, the flattening of the particle during its impact, determines coating thermo-mechanical properties (Ref 1). Thus, the spreading and cooling of fully melted droplets upon impact on a rigid smooth surface have been studied by many researchers either by numerical (Ref 2) and analytical modeling (Ref 3) or by sophisticated experimental techniques (Ref 1).

Upon impact, liquid droplets flatten and solidify; solidification starting before flattening is completed. The resulting splat shapes can vary from disk to extensively fragmented shapes. To understand the complex phenomena involved in these processes, it rapidly became evident that the fast pyrometers (50 ns response time) used since the nineties to study them, were not sufficient. To interpret the signals obtained, the flattening process must be followed in parallel. However to follow the flattening process in spray conditions, cameras able to take at least five pictures per microseconds (or more), should be used. Unfortunately, they do not exist yet (Ref 4). To overcome the lack of very fast cameras, a setup has been developed where an Nd-YAG laser emitting a 5-ns pulse provides illumination for a CCD camera to photograph the impacting droplet (Ref 5). Thus assuming that it is possible to produce successive impacting particles with the same impact parameters, it becomes possible, by triggering the camera at different times, to follow the particle flattening (Ref 5). In parallel with the experimental studies started in the nineties on micrometer-sized particle flattening, experiments were developed with millimeter-sized ones. With such particles, flattening times are increased by about three orders of magnitude and thus camera with 3000-15,000 frames/s can be used to follow particle flattening. The problem of the comparison of such millimeter-sized particles with micrometer-sized ones is twofold:

- millimeter-sized particles are produced in furnaces which implies using metals (and not refractory ones) or alloys and, of course, not ceramics. To solve this problem, Nagashio et al. have used an aerodynamic levitator (ADL) in order to melt a YAG powder and

This article is an invited paper selected from presentations at the 2009 International Thermal Spray Conference and has been expanded from the original presentation. It is simultaneously published in *Expanding Thermal Spray Performance to New Markets and Applications: Proceedings of the 2009 International Thermal Spray Conference*, Las Vegas, Nevada, USA, May 4-7, 2009, Basil R. Marple, Margaret M. Hyland, Yuk-Chiu Lau, Chang-Jiu Li, Rogerio S. Lima, and Ghislain Montavon, Ed., ASM International, Materials Park, OH, 2009.

S. Goutier, M. Vardelle, J.C. Labbe, and **P. Fauchais**, SPCTS Laboratory, Limoges, France. Contact e-mail: simon.goutier@unilim.fr.

Table 1 Few values of dimensionless numbers

	Micrometer-sized droplet (10 μm) $v_{particle} = 220$ m/s	Millimeter-sized drop (5 mm) $v_{particle} = 5$ m/s	Millimeter-sized drop (5 mm) $v_{freefall} = 3$ m/s + $v_{piston} = 7$ m/s
Re	160	1812	3600
We	2183	564	2200
Pe	105	1187	2370

to form a drop with a diameter of about 3.5 mm, and next to study its flattening with an impact velocity of 1 m/s (Ref 6).

- the maximum particle velocities are those of free falling experiments (below about 5 m/s) (Ref 7, 8).

Thus, it is difficult with millimeter-sized droplets to achieve dimensionless numbers (Reynolds Re, Weber We, Peclet Pe, and Stephan St) identical to those obtained with micrometer-sized particles. For example, an impact velocity of 5 m/s for a 5 mm drop of alumina corresponds to We = 564 while with a 10 μm drop of the same material impacting at 220 m/s, We = 2183 (see Table 1). To solve the problem of particle velocity, Mehdizadeh and co-workers have developed a setup where millimeter-sized drops of tin are accelerated up to 30 m/s by a rotating plateau (Ref 9, 10). Using a relative velocity to increase the impact velocity (v_p), is a good idea because the free fall particle time is reduced and it can be obtained with a wide velocity variation. Thus, for a given sprayed material at a given temperature, an important variation of Weber number is obtained. The setup described below has been developed to produce alumina drops with velocities up to 10 m/s. First, the drop generator and the measuring devices associated will be presented, then a few examples of results will be given.

2. Experimental Setup

2.1 The Drop Generator

The system to produce liquid ceramic drops (Fig. 1) is composed of a revolving graphite crucible heated by a transferred arc. To avoid its oxidation, the crucible is located in a small chamber filled continuously with argon (Pressure = 120 × 10^3 Pa), in order to keep the inert atmosphere in spite of the hole in bottom the crucible. Inside the crucible, an alumina cylinder, 4 mm in diameter and 4 mm in length, is introduced to be melted.

The crucible shape (see Fig. 1) is such that the liquid material is directed out through a hole bored at the crucible bottom, where a discontinuity prevents liquid alumina spreading at crucible exit. At this exit a suspended drop is established, which detaches when the gravity force overcomes its surface tension force. The flow through the hole is governed by the pressure difference between the crucible top and the hole exit. Thus by introducing a slight overpressure at the top, thanks to a sharp increase of the

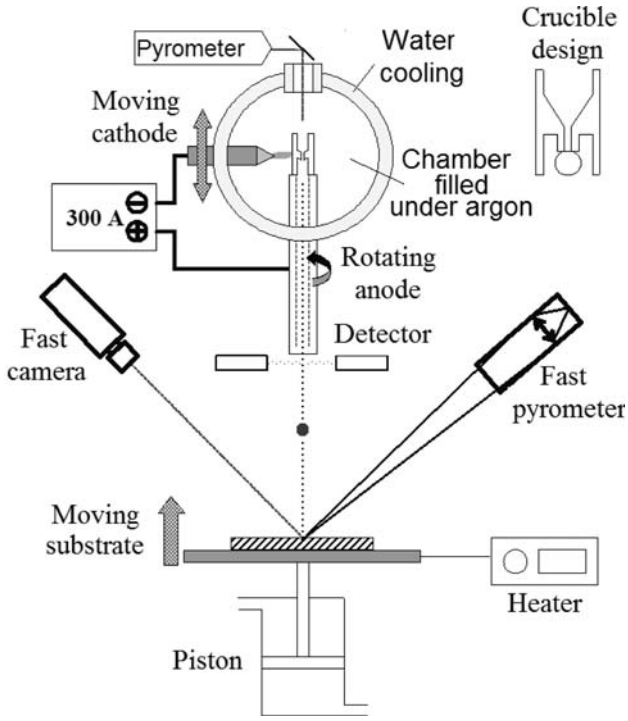

Fig. 1 Drop generator principle

gas mass flow rate, it becomes possible to accelerate the flow and thus decrease the alumina contact time with the crucible. The time necessary to melt the alumina rod piece and obtain a drop in free fall is approximately 8 s with a generator power of 5.8 kW. When the drop starts falling, its temperature is close to 2200 °C (±50 °C), and its cooling is about 80 °C (±20 °C) for a free fall of 1.5 m. A detector allows the generation of one TTL pulse (5 V) when the drop starts falling.

To give a high impact velocity to the drop, the substrate is placed at the top of a pneumatic piston whose velocity can reach up to 7 m/s. When the particle has reached a given position, a solenoid valve is opened and the piston starts moving up in order to impact the free fall drop at a given location and so the impact velocity of the drop is its free fall one plus that of the piston.

2.2 The Measuring System

The dichromatic pyrometer (50 ns of response time) (Ref 11) targeting the impact location, collects the thermal radiation emitted by the flattening drop. The pyrometer optic is such that the field depth is a few centimeters corresponding to the substrate displacement amplitude. The measuring area is a disk about 15 mm in diameter, and the pyrometer targets the impact location. The measuring area is defined by the maximum flattening diameter of the splat in order to measure a mean temperature. Signals are filtered by a monochromator (H10IR-Jobin-Yvon with holographic gratings, 600 grooves/mm, and a bandwidth of 16 nm) at two different wavelengths (565 and 630 nm).

Both signals obtained are then transmitted, by optical fiber, to two photomultipliers (Hamamatsu R928). A National Instrument interface allows the fast acquisition (4000 Hz) of signals, and the data processing is performed under Labview®.

The pyrometer calibration was made by using a tungsten lamp, and an alumina rod locally melted by a blown d.c. arc plasma torch to precisely measure the melting point of alumina.

The fast camera used is a FastCam 1024 PCI from Photron®. For this study, the imaging frequency is between 4000 and 15,000 Hz. The angle between the camera axis and the furnace axis is 30°. To follow the flattening during the piston displacement, the focus distance is 120 cm (field of depth of a few centimeters). In this condition, the number of pixel is 384 × 608 and the windows measures 46 × 73 mm^2. All photographs are made with only the radiation from the alumina. No lighting is used, because the radiation of alumina is very important. However in some cases, the thin splat area cooling faster than the thicker area, can be missed by the camera. In such cases, the camera aperture is modified to observe the less emitting area, but then the signal of the very hot central part is saturated.

With these two measuring setups, it becomes possible to correlate at the same times the signal emitted by the particle, its temperature and its instant 2D shape during flattening.

A low frequency pyrometer (20 Hz) is used to follow the melting of the alumina rod into the crucible.

2.3 Preparation of Substrates

The stainless steel substrates (304L) are mirror polished by using SIC paper 4000. Substrates are fixed on copper supports heated by two small resistances (150 W dissipated in each of them) up to 693 K with a heating velocity of 0.5 K/s

3. Results

3.1 Influence of Weber Number

Figure 2 shows images of 5 mm alumina drops impacting on the mirror-polished stainless steel substrate with different velocities (up to 10 m/s when the piston is used ($v_{freefall} = 3$ m/s, $v_{piston} = 7$ m/s)). The last column corresponds to hot substrate ($T_s = 693$ K), while the others are related to cold substrates ($T_s = 293$ K). The study of the spreading on cold substrates of drops with different impact velocities shows that when the Weber number increases (D1 to D3), as it can be expected, the particle tends to better spread out. As the contact with the substrate is rather poor at room temperature, the flattening particle spreads out faster when the impact velocity increases. It creates a thin film of alumina, which is almost transparent, except at its fringes where a rim is formed. This thicker rim emits more light than that of the film connecting it to the particle central part, which is constituted of part of the drop initial volume. It is also interesting to underline that when the Weber number is <500, the matter starts to recoil toward the splat center (see Fig. 2, D1 case, $t = 3.2$ ms), because, due to the poor contact flattening-drop substrate, there is no solidification and at the end of the recoiling matter movement, a sphere is obtained and not a splat. To obtain splats, it is necessary to achieve Weber numbers over 500. This phenomenon is due to the fact that during the initial rapid deformation stage (Fig. 2, D1 case, $t = 0$-1.6 ms) the inertial strength of impact is much larger than the viscous strength. However,

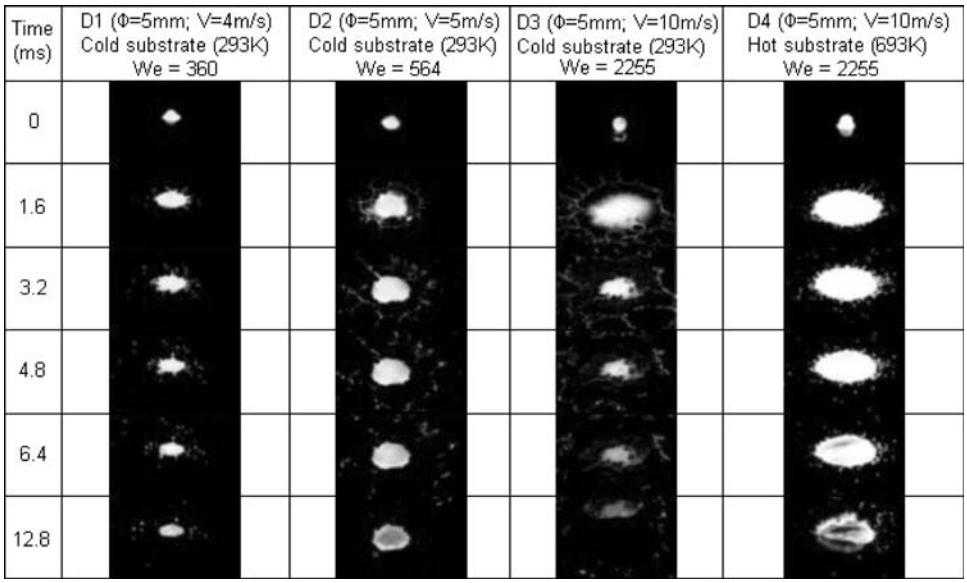

Fig. 2 Alumina drop flattening on polished stainless steel for different impact velocities (D1 to D3), and for two different substrate temperatures at the same Weber number (D3, D4), where Φ is the particle diameter and V the impact velocity

when the droplet approaches the maximum extent, the spreading velocity decreases and the viscous effect begins to play the dominant role (Ref 12) and so the matter recoils toward the center. When the velocity increases, there is a rise in viscous dissipation attributed to wall shear stress on the extended area of liquid-solid contact (Ref 12) and also maybe a better thermal contact splat-substrate limiting the recoil phenomenon.

In the case of a Weber number close to that of the plasma conditions, D3 (when piston is used), it can be noted that the particle spreads out more, and also cools down faster, which is probably due to the less important mass of its central part, as well as the better contact flattening drop substrate. This cooling down is such that, according to the pyrometer measurements, the central part surface is solidified when the piston arrives at the end of its race (12.8 ms after the impact). Splashing is due to the rupture of the thin film expanded around the central part of the splat (Fig. 2, D3 case, at about 3.2 ms). In addition, the splat obtained does not adhere sufficiently to resist at the abrupt deceleration of the piston, when reaching the end of its run, and it detaches (Fig. 2, D3 case, at 12.8 ms). On a preheated surface, the particle undergoes a different flattening splashing phenomenon in spite of its high Weber number. Indeed, it can be observed (see Fig. 2, D4 case) that there is no thin film expanded around the splat center. Therefore, it can be supposed that flattening is impeded by the splat solidification at substrate surface and the splashing observed is due to the liquid droplets jetting out at its surface (Ref 13). When the piston arrives at the end of its race, the splat center is freezing and splat edges are still liquid. The splat center (Fig. 2, D4 case, dark area at 12.8 ms) adheres well to the substrate. So there is a real difference between hot and cold substrate. To explain this difference, the correlation between flattening pictures and pyrometer signals is needed.

3.2 Correlation Between Flattening Pictures and Pyrometer Signals

To explain the particle flattening, the fast pyrometer is used. Figure 3 shows images of 5 mm diameter alumina drops impacting on a mirror-polished stainless steel substrate for the same impact velocity (5 m/s). Figure 4 corresponds to the pyrometer signals recorded for drop D5 (hot substrate) and D7 (cold substrate) at the wavelength of 630 nm. It can be noted that both particles undergo undercooling phenomenon during flattening and the lower temperature for this undercooling is reached when particles are at their maximum extents (at about 2-4 ms). Then, due to crystallization, the temperature increases up to the solidification plateau. The case of the alumina drop

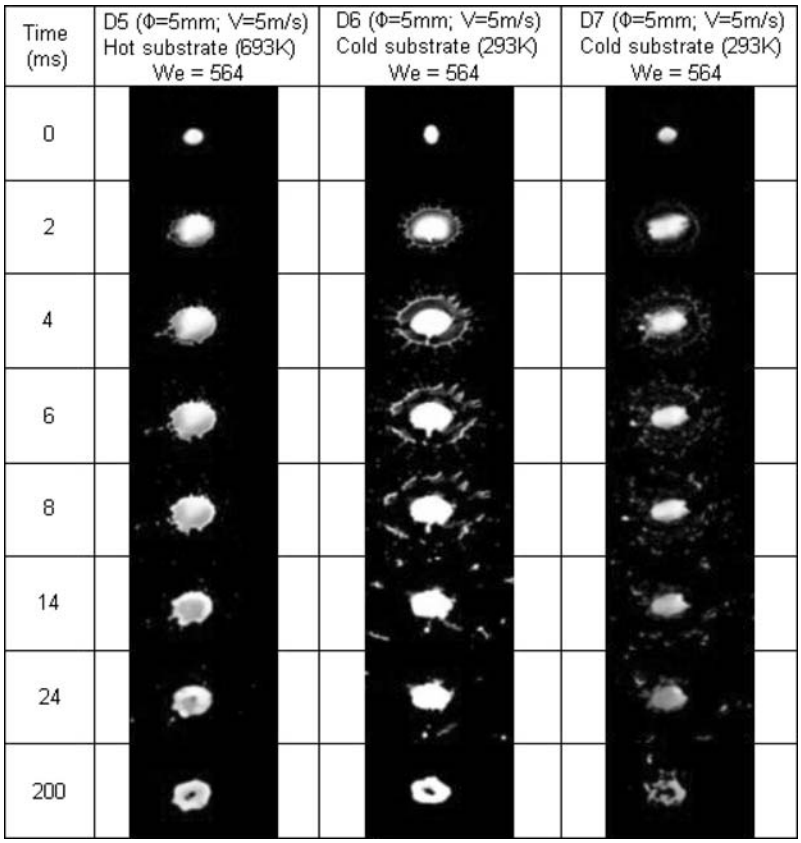

Fig. 3 Alumina drop flattening on stainless steel substrate for two camera apertures (D6, D7), and for two substrate temperatures (D7, D5), where Φ is the particle diameter and V the impact velocity

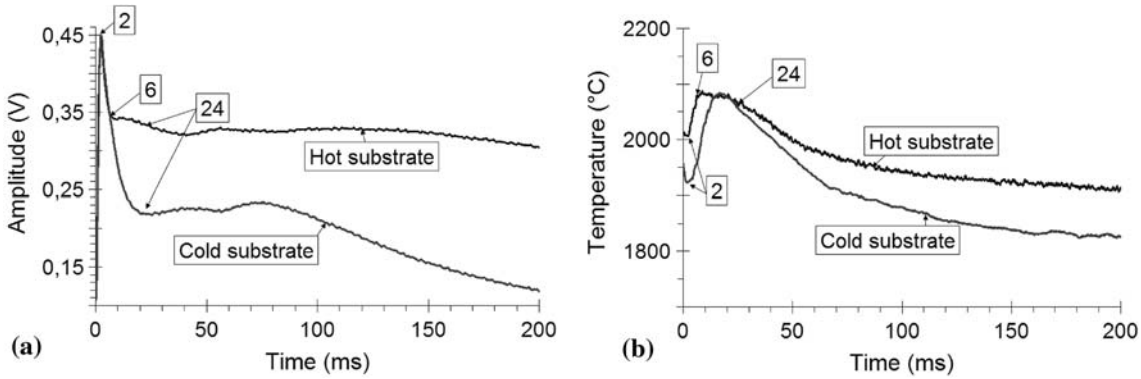

Fig. 4 (a) Pyrometer signals ($\lambda = 630$ nm) and (b) temperature time evolution for cold (293 K, case D7 in Fig. 3) and hot (693 K, case D5 in Fig. 3) substrate. Numbers correspond to times of some pictures in Fig. 3

impacting with a velocity of 10 m/s is not presented because when the piston is used, it becomes difficult to record all the particle signals due to the very short measuring time at the end of impact (up to 13 ms) and so it is not possible to follow the whole particle cooling.

3.3 Hot Substrate

For the splat on a hot substrate (D5 case), the thermal contact is much better (desorption of adsorbates and condensates) and the cooling begins before that of the same splat on a not preheated surface. The liquid remains at the splat surface and during flattening this liquid tends to migrate toward splat edges and form a rim, clearly visible in Fig. 3 (D5 case at 6 ms). Later on when the flow parallel to the substrate is terminated, the surface tension takes over bringing back the liquid toward the splat center (between 8 and 24 ms), modifying locally the splat thickness and splat surface (Ref 12). And so the pyrometer sees more emitting surface, which results in a slight increase of the pyrometer signal at 14 ms (Fig. 4a). Later on, there is a slight increase of particle signal (at about 50 ms) due to the solidification of this recoiled matter. However, on particle temperature evolution (Fig. 4b), it can be seen that at 50 ms the temperature signal is decreasing. No temperature increase is observed for splat edges due to their solidification. This effect is due to the large measuring volume inducing a global temperature measurement.

3.4 Cold Substrate

On the contrary, the splat on a cold substrate solidifies later, and the solidification plateau is shorter than in the case of a hot substrate (see Fig. 4). This phenomenon can be explained thanks to the flattening images of two different drops D6 and D7. They have the same diameter and same impact velocity. The only difference comes from the camera diaphragm aperture (9 for D6 and 11 for D7). The advantage of having amended the diaphragm aperture is that it allows saturating the splat center and permits the observation of the splat fringes, which otherwise would be black as on the D7 images. However, the information about the central part is also necessary and the parallelization of these two drops is essential to understand the phenomena. To explain better the impact phenomenon, in Fig. 5(a), there is different pictures snap at different times of the flattening on a cold surface for a 5-mm diameter alumina drop with an impact velocity of 5 m/s. The fast camera is directed perpendicularly to the falling drop trajectory and in this case the imaging frequency is 10,000 frames/s. In Fig. 5(b), a schematic view, deduced from the all recorded images, aids the understanding of the flattening of a drop on a cold surface. The conclusions are that at the impact the splat develops a liquid crown propagating with a higher speed (15 m/s) compared to that of the overall propagation of the splat (close to 10 m/s). Indeed at the impact, the desorption of condensates and adsorbates creates a high degassing and so a vapor cloud appears between flattening matter and substrate (Ref 14). Also a small amount of matter is ejected (Fig. 5a, $t = 0.1$ to 0.2 ms) and a peripheral ring is formed (Fig. 5a, $t = 0.3$ ms) and propagates on the surface to form a crown (Fig. 5a, $t = 0.7$ ms and (b), picture 3). However, an important part of the initial drop is not yet flattened. This matter then flattens on the already solidified crown (Fig. 5b, picture 3, zoom view). Therefore, the friction strengths are higher and the flattening velocity is less than in the case of the peripheral ring flattening. The crown is solidified because this thin film spreading out covers a large surface radiating proportionally and having also a large contact with the ambient air, conditions promoting fast solidification (Fig. 3, D6 case, at 4 ms). At the maximum extent, due to the kinetic energy of the liquid, a second ring is formed at the central part edges (Fig. 5b, picture 5) and so it locally melts the crown and finally, this thin film tends to separate from the central part of splat (Fig. 3, D6 case, at 6 ms, and Fig. 5b, picture 6), which induces the decrease of the particle radiation (Fig. 4a, cold substrate). However, a weak part of the splat remains liquid, inducing the light bump on the signal emitted by the particle during the spreading out of this fluid (at about 40 ms). Later on (at about 70 ms), it can be observed the splat edges crystallization. At 200 ms, it can be noted that the particle cools more quickly at the impact location.

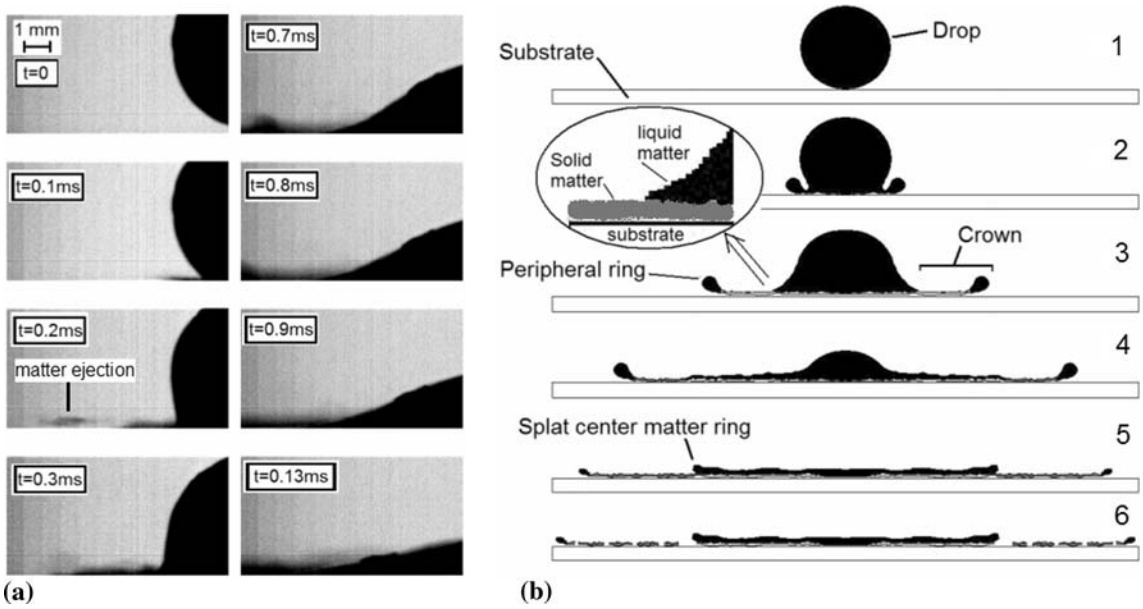

Fig. 5 Alumina drop flattening on cold stainless steel substrate (293 K) (a) real view of drop impact location and (b) schematic view of the flattening

To summarize, when comparing the case on a cold substrate with that on a hot surface it is important to note that after the maximum extents, there is a lot of matter lost on the cold substrate and there is a large radiating surface. So the cooling rate on the cold substrate is higher, but the thermal contact is probably less than on a hot substrate. Indeed the thermal transfer is made through a vapor cloud. For a better understanding of the phenomena involved, the examination, at different substrate temperatures, of the splat bottom surface could be useful.

3.5 Study of Splat Bottom Surface

In the case of a hot substrate (693 K) for a drop speed of 5 m/s, on almost the whole surface a dense microcrack network can be observed (Fig. 6a). For a cold substrate (293 K), and the same impact parameters, and on almost the whole surface, the presence of a star-type fracture network can be seen (Fig. 6b). This difference in microstructures cannot be explained without deeper analyses. However, it can be assumed that the contact with the hot substrate (693 K) is rather good on most of the splat surface, whereas in the case of a cold substrate (293 K), only a few good contact points with the substrate exist, corresponding probably to the star fractures, the remainder of the splat being isolated from the substrate by gas pockets.

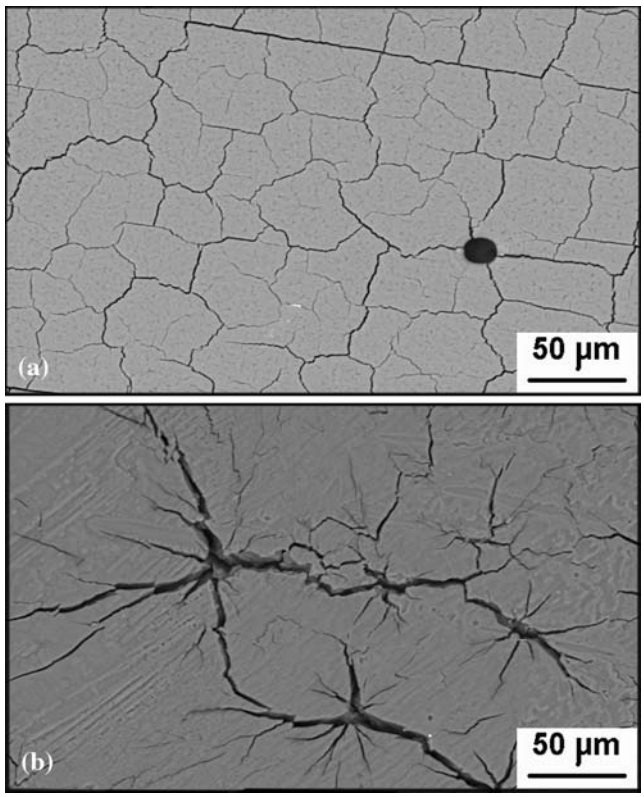

Fig. 6 Alumina splat bottom near the splat center: (a) hot substrate (693 K) and (b) cold surface (293 K)

4. Conclusion

In this study, a new process has been presented. Fully melted alumina millimeter-sized drops can be produced with impact velocities up to 10 m/s. This highly reproducible experimental setup is composed of revolving graphite crucible heated by a transferred arc and of a vertical moving piston used to increase the drop impact velocity

(up to 10 m/s). The results presented in this paper are first ones, but already interesting.

The system allows:

- following the drop flattening with an impact Weber number close to that obtained in plasma spraying of micrometer-sized particles.
- observation of the interface between splat and substrate. In the case of a cold substrate, small contact areas (about 10 μm in length) are observed. At these points, the stress release induces star-shaped cracks. On the contrary, for a hot substrate, an interconnected microcrack network (40 μm in mesh) can be observed.

For future work, it is intended to analyze finely the splat interface microstructure and measure the thermal contact resistance between splat and substrate.

References

1. P. Fauchais, M. Fukumoto, A. Vardelle, and M. Vardelle, Knowledge Concerning Splat Formation: An Invited Review, *J. Therm. Spray Technol.*, 2004, **13**, p 337-360
2. M. Pasandideh-Fard, S. Chandra, and J. Mostaghimi, A Three-Dimensional Model of Droplet Impact and Solidification, *Int. J. Heat Mass. Trans.*, 2002, **45**, p 2229-2242
3. M. Lesser, Analytic Solutions of Liquid-Drop Impact Problems, *Ann. Rev. Fluid Mech.*, 1981, **377**, p 289-308
4. K. Shinoda, H. Murakami, S. Kuroda, S. Oki, K. Takehara, and T. Etoh, High-Speed Thermal Imaging of Yttria-Stabilized Zirconia Droplet Impinging on Substrate in Plasma Spraying, *Appl. Phys. Lett.*, 2007, **90**, p 194103/1-194103/3
5. N. Mehdizadeh, M. Lamontagne, C. Moreau, S. Chandra, and J. Mostaghimi, Photographing Impact of Molten Molybdenum Particles in a Plasma Spray, *J. Therm. Spray Technol.*, 2005, **14**, p 354-361
6. K. Nagashio, K. Kodaira, K. Kuribayashi, and T. Motegi, Spreading and Solidification of a Highly Undercooled $Y_3Al_5O_{12}$ Droplet Impinging on a Substrate, *Int. J. Heat Mass. Trans.*, 2008, **51**, p 2455-2461
7. M. Fukumoto, E. Nishioka, and T. Matsubara, Flattening and Solidification Behavior of a Metal Droplet on a Flat Substrate Surface Held at Various Temperatures, *Surf. Coat. Technol.*, 1999, **120-121**, p 131-137
8. J. Cedelle, M. Vardelle, and P. Fauchais, Influence of Stainless Steel Substrate Preheating on Surface Topography and on Millimeter- and Micrometer-Sized Splat Formation, *Surf. Coat. Technol.*, 2006, **201**, p 1373-1382
9. N. Mehdizadeh, M. Raessi, S. Chandra, and J. Mostaghimi, Effect of Substrate Temperature on Splashing Molten Tin Droplets, *J. Heat Trans.*, 2004, **126**, p 445-452
10. R. Dhiman and S. Chandra, Freezing-Induced Splashing During Impact of Molten Metal Droplets with High Weber Numbers, *Int. J. Heat Mass Trans.*, 2005, **48**, p 5625-5638
11. J. Mishin, M. Vardelle, J. Lesinski, and P. Fauchais, Two-Colour Pyrometer for the Statistical Measurement of the Surface Temperature of Particles Under Thermal Plasma Conditions, *J. Phys. E Sci. Instr.*, 1987, **20**, p 620-625
12. A. Yarin, Drop Impact Dynamics: Splashing, Spreading, Receding, Bouncing, *Ann. Rev. Fluid Mech.*, 2006, **38**, p 159-192
13. R. Dhiman and S. Chandra, Freezing-Induced Splashing During Impact of Molten Metal Droplets with High Weber Numbers, *Int. J. Heat Mass Trans.*, 2005, **48**, p 5625-5638
14. X. Jiang and Y. Wan, Role of Condensates and Adsorbates on Substrate Surface on Fragmentation of Impinging Molten Droplets During Thermal Spray, *Thin Solid Films*, 2001, **385**, p 132-141